3rd International Conference on Advances in Civil and Environmental Engineering (ICACEE-2024)

University of Engineering & Technology Taxila, Pakistan

Conference dates: 21st and 22nd February 2024; ISBN: 978-969-23675-2-3

Sloping Perspectives: Investigating Flow Hydrodynamics in Vegetated Open-Channels under Varying Bed Slope

Nadir Murtaza[1,*], Ghufran Ahmed Pasha[1], Ahmed Murtaza[2], Afzal Ahmed[1], Hammad Raza[1], Muhammad Ashraf Khalid[1]

[1]Civil Engineering Department, University of Engineering and Technology Taxila, Pakistan

[2]Center for Disaster Preparedness and Management, University of Peshawar Pakistan

*Corresponding author: nadirkhattak1122@yahoo.com

ABSTRACT

Vegetated open channels play a crucial role in shaping the dynamics of riverine ecosystems. This study, conducted in two distinct phases under sub-critical flow conditions, aimed to understand the impact of altering the channel bed while maintaining a constant flow discharge. In the initial phase, a vegetated open channel, featuring vegetation followed by a moat, was utilized to experimentally investigate hydrodynamic parameters such as the reduction of fluid force (*RFI%*), moment index (*RMI%*), and overflow volume ($\Delta Q\%$). Moving to the second phase, an artificial neural network (*ANN*)-based model incorporating six and nine different neurons was applied to the experimental data. The experimental results show that *RFI%* and *RMI%* enhanced with enhancing *Fr* from 0.35 to 0.65. It was noticed that the maximum *RFI%* and *RMI%* were 72.84% and 69.39% when Froude number reached at 0.65 for vegetation followed by a moat (VM) respectively. It was noticed that $\Delta Q\%$ decreased with enhancing the *Fr*. The maximum value of $\Delta Q\%$ was noticed to be 44.98%. The ANN model yielded superior results with increased coefficients of determination (R^2) and Nash-Sutcliffe efficiency (NSE) when configured with nine neurons in each hidden layer. Conversely, it exhibited reduced values for root square mean error (RSME), sum of square error (SSE), and mean absolute error (MAE). The finding of the study concluded that varying channel bed slopes have a greater influence on the reduction of hydrodynamic parameters.

KEYWORDS: Vegetated open channel, artificial neural network, overflow volume, statistical analysis.

1 INTRODUCTION

Vegetation, a fundamental component of rivers in their natural states, is a major factor Vegetation has several positive effects on ecosystems, but it also has negative effects on flow resistance and sediment transfer. As a result, river stretches are typically required to have their vegetation managed from an engineering perspective to minimize the likelihood of flooding [1]. To investigate the hydraulics of flow and their characteristic in open channel vegetation have been widely used [2-5]. Previous research examined the energy reduction phenomenon through emergent vegetation [5,7].

Numerical research on flow hydrodynamics in a compound channel has also been conducted [8]. Vertical double layered and discontinuous vegetation patch was examined numerically in an open channel for investigating turbulence flow structure [9]. In real world floodplain and the prototypes main channel flow have different effects, and these differences have been studied experimentally to evaluate the reduction of flow energy through vegetation by measuring the drag coefficient and three-dimensional velocity [10,11]. Previous research has evaluated the flow resistance owing to floodplain vegetation and analysed fluvial processes through floodplain vegetation in two dimensions [5]. Similarly, Sanjou et al. [11] experimented to determine the effectiveness of a single tree line in reducing flood energy under sub-critical flow, and they derived an equation for energy reduction, including two parameters: the density of vegetation and the Froude Number (Fr). The influence of riparian vegetation abundance on variations in flow rate inside the canopy of vegetation was investigated and the result shows that flow velocity increases by increasing the vegetation density at the main channel while decreasing at the riverbank [12].
Over the past decades, different scholars have examined flow characteristic using prototypes such as vegetation, embankment, and combination of both [13],[14], simulation techniques [15], and systematic methodologies [16], [17]. There is a concern that damages caused by floods increase in the future [18], [19]. In some cases, extreme flow conditions have resulted in destruction of embankments, coastal vegetation, flood mitigation obstruction, and infrastructure [20], [21], [22]. Different constructional strategies encompass various structural interventions, such as the establishment of reservoirs, barriers, raised structures, watercourse dredging, and implementation of flood-resistant buildings [23], [24]. Additionally, non-structural measures such as disaster preparedness, and advance alert devices are considered as potential choices. However, the limitations of these strategies in effectively utilizing flood resources have led to the recognition and emphasis on a coordinated approach to water resources management [25]. At present, there is growing recognition of the significance of ecological and natural approaches in both advanced and developing nations [26]–[29].
Previous studies shows that flow characteristic on the upstream and downstream side of the vegetation was investigated under constant channel bed slope and varying discharge. However, the present aimed to investigate flow characteristic on the downstream side of the vegetation by altering channel bed slope and keeping flow discharge constant. Therefore, the present study investigates hydrodynamic parameters such as the reduction of fluid force (*RFI%*), moment index (*RMI%*), and overflow volume ($\Delta Q\%$) experimentally in the first phase. In the second phase, ANN-based model was run to determine the predicted values of hydrodynamics parameters under different number of neurons in two different model (a model with six and nine neurons in hidden layer respectively).

2 METHODOLOGY

2.1 Flow Conditions

Pakistan has a long history of floods from 1947 to 2022 [5]. It has been observed that along the Indus River, mostly in plain domains, the floods are mostly sub-critical. Therefore, to replicate the sub-critical flow conditions in a channel, the discharge data spanning 59 years (1961 to 2020) was collected from the Federal Flood Commission. This data pertained to the Froude number at two locations along the Indus River: Jinnah Barrage (upstream) and Taunsa Barrage (downstream). The Froude number is defined as the ratio of inertial forces to gravitational forces ($Fr=V/(gy)^{0.5}$, where V is the depth-average velocity in a flume without any obstruction, y is the water depth without obstructions, and g is the gravitational acceleration. According to the FFC report, the Fr_o during floods ranged between 0.07-0.89[5]. Therefore, in the present investigation the discharge remained constant, and the bed slope was increased from 1/100 to 1/450, resulting in the Froude number from 0.35 to 0.65 (Table 1). Therefore, in the current study, seven different Froude numbers (0.35-0.65) were selected in a flume without placing any barrier. Experimental and hydraulic conditions of the present study are summarized in Table 1. *Figure 1a* depict the schematic diagram of the channel with a moat and vegetation model. In Figure 1a, Point G was taken as a reference point on the downstream side of the vegetation to measured water depth and flow velocity. The water depth and flow velocity at Point G were used for measuring the values of *RFI%, RMI%* and $\Delta Q\%$.

Table 1: Experimental and Hydraulic conditions of present research

Run	Fr	y (cm)	Wv (cm)	d (m)
1	0.35	8	38	0.003
2	0.40	7.5	38	0.003
3	0.45	6.7	38	0.003
4	0.50	6.3	38	0.003
5	0.55	5.9	38	0.003
6	0.60	5.5	38	0.003
7	0.65	5.3	38	0.003

2.2 Vegetation and Moat Conditions

Eucalyptus trees are the most common type of vegetation planted in the southern region of Punjab, Pakistan. Locally, the Eucalyptus tree is known as Sufaida, and by nature, it requires a greater amount of water for its growth. In the southern region of Punjab, Pakistan, Eucalyptus trees can be seen in the floodplain to maximize the interception rate and reduce flow velocity to enhance the resilience of the local community against extreme flood conditions. The average trunk diameter of the Eucalyptus tree is 0.11 -0.33m and the average height is in the range of 4.7-11.4m [30]–[32]. In the southern region of Punjab, Pakistan vegetation is planted at a spacing (G) of 6 m between them with an average trunk diameter (d) of 0.11-0.33 [31]. However, in our study, we opted for cylindrical rods made of steel with average diameter of 3 mm at scale of 1/100. We also introduced a sparse vegetation configuration with a density of 2.13. The density was defined by the G/d ratio, where G is the gap between two adjacent vegetation elements and d is the diameter of the vegetation element (*Figure 1c*).

Moats could be either dry or filled with water, depending on the availability of water sources and the specific defensive requirements of the structure. Moat is often created to safeguard specific areas, such as buildings, homes, or entire communities, from the potentially damaging effects of flooding. The purpose of a flood moat is to act as a drainage system or a defensive barrier against rising water levels. The scale of 1/100 was chosen to model the moat, considering the optimal height of a wall (embankment) on the Indus River in Pakistan, which typically falls in the range of 4-7 meters, along with an additional 1.2-1.8 meters of freeboard [5,33]. For the present research, a moat depth of 6 meters was selected. This led to the elevation of the moat prototype being set at 6 cm using the 1/100 scale. *Figure 1b* depicts the scaled-down characteristics of the moat. During flood events, the water travels in an inclined direction relative to the main channel from the wall across the flooded area. The direction of the flowing water approaching an embankment-like barrier in the watercourse flood can take different pathways, such as at right angles or inclined according to the orientation of the installation of the barrier [31,32]. For this study, it is assumed that the terrain's barrier will be situated in a manner that the water movement is at right angles to the barrier.

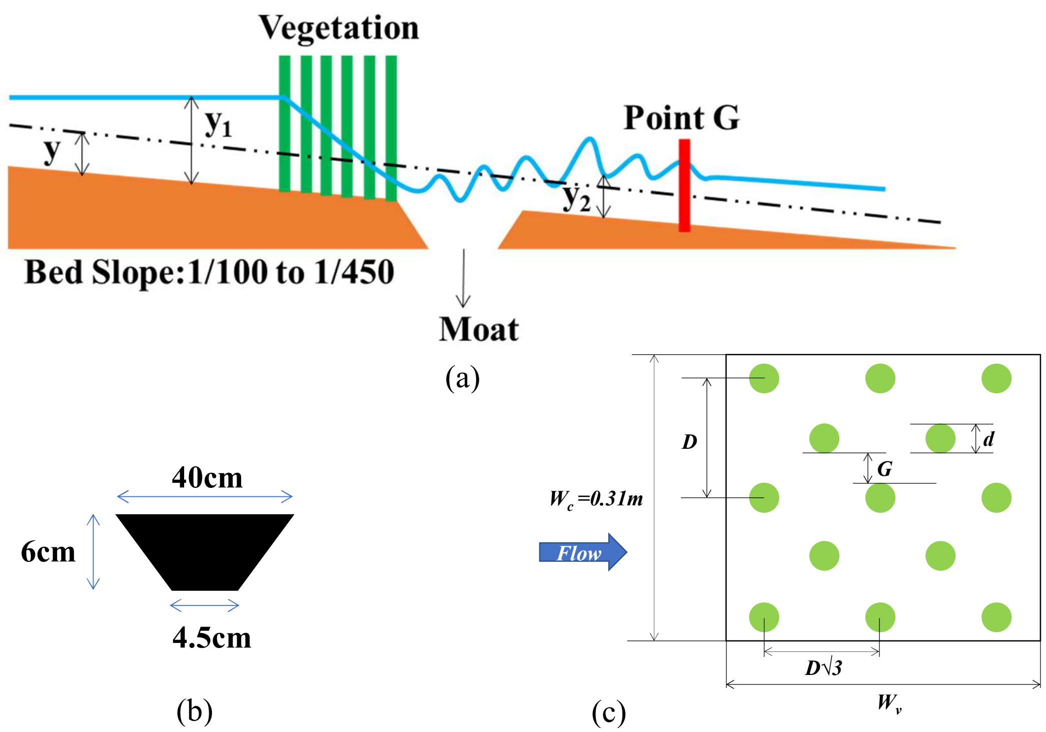

Figure 1. (a) Schematic diagram of the channel and laboratory investigation (b) moat specifications (c) vegetation conditions and parameters definition.

2.3 Artificial Neural Network Model (ANN) Model Evaluation Criteria

An artificial neural network consists of interconnected nodes, or artificial neurons, organized in layers. These layers include an input layer, one or more hidden layers, and an output layer [34]. Each connection between nodes has an associated weight, and the network learns by adjusting these weights based on input data [34]. A feed-forward network having layers of neurons that comprise input, hidden, and output layers is known as a multilayer perceptron (*MLP*). To assign input messages to neurons in the hidden layer, neurons in the input layer buffer the signals. *Figure 2* depicts the feed-forward ANN model's flow chart. Statistical measures including root means square error (*RSME*), coefficient of determination R^2, the Nash Sutcliffe model efficiency, sum of square error (*SSE*) and mean absolute error (*MAE*) was evaluated to check the performance of ANN model. For measuring the statistical measure Froude number vegetation density, and ratio of moat length to initial water depth was considered as input. Equations below show the formulae of finding this statistical measure such as R^2, *RSME, SSE*, *MAE*, and *NSE*.

$$R^2 = \frac{\left(\sum_{i=1}^{n}(C_i - \bar{C})(C_i{}' - \bar{C}')\right)^2}{\sum_{i=1}^{n}(C_i - \bar{C})\sum_{i=1}^{n}(C_i{}' - \bar{C}')^2} \quad (1)$$

$$RSME = \sqrt{\frac{\sum_{i=1}^{n}(C_i - C_i{}')^2}{n}} \quad (2)$$

$$SSE = \sum_{i=1}^{n}(C_i{}' - \bar{C})^2 \quad (3)$$

$$NSE = 1 - \frac{\sum_{i=1}^{n}(C_i - C'_i)^2}{\sum_{i=1}^{n}(C_i - \bar{C})^2} \quad (4)$$

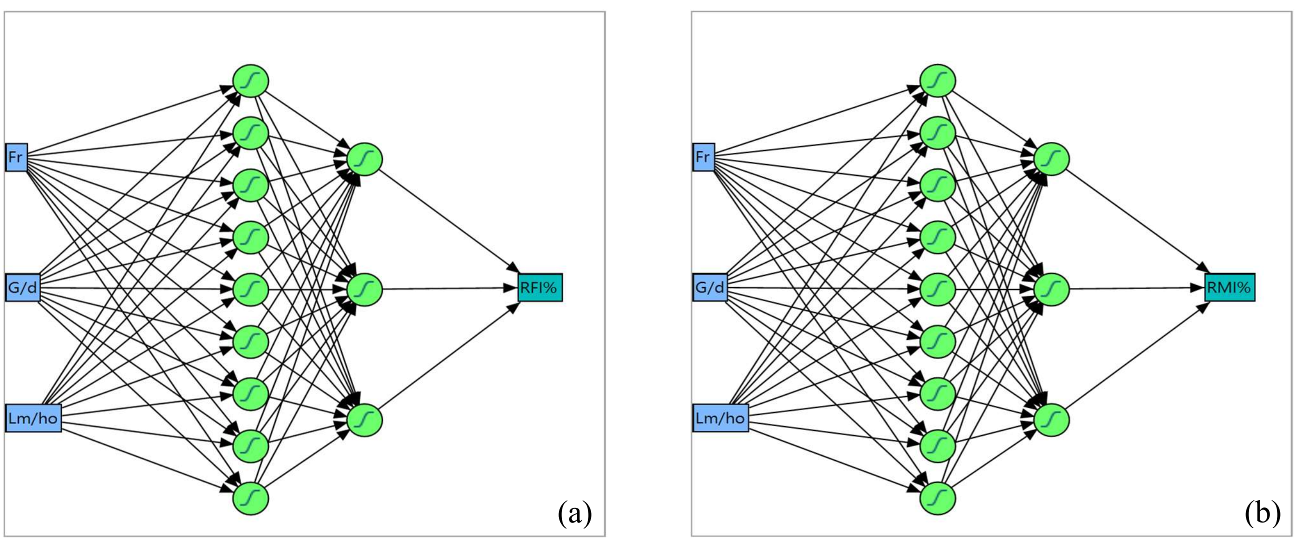

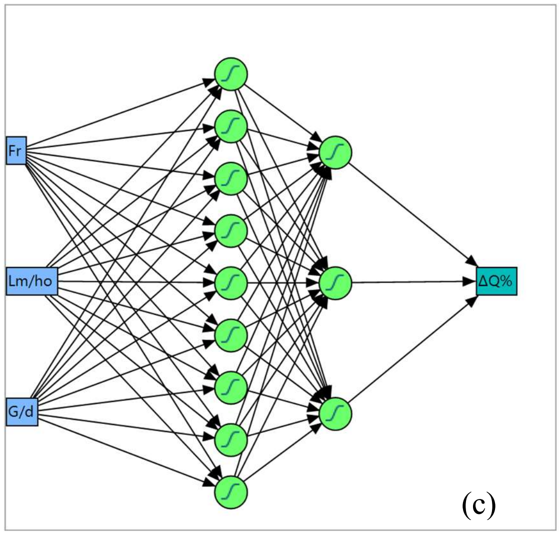

Figure 2. Feed-forward ANN-Mode diagram with different neurons in hidden layer to predict values of different indices (a)RFI% (b) RMI% (c) ΔQ%.

3 RESULTS AND DISUCSSION

3.1 Experimental Results of RFI%, RMI%, and ΔQ%

The maximum reduction of fluid force index (*RFI%*), moment index (*RMI%*) and overflow volume(Δ*Q%*) were calculated against seven different Froude number (*Figure 3*). It was noticed that *RFI%* increased by increasing the Froude number from 0.35 to 0.65 (*Figure 3*). The maximum *RFI%* noticed was 72.84% when values of the Froude number reached to 0.65. The increased in *RFI%* with Froude number was because of greater flow velocity at Point G (*Figure 1a*) due to the formation of hydraulic jumps on the downstream side of the vegetation. Similarly, *RMI%* was noticed to be increased by increasing Froude number (*Figure 3*). The maximum *RMI%* noticed was 69.39% when Froude number increased to 0.65. The increase in *RMI%* with increasing Froude number was because of increased in energy reduction due to formation of hydraulic jump result in greater *RMI%*. The maximum Δ*Q%* was noticed 45% when Froude number reached to 0.65. It was noticed that Δ*Q%* decreased by increasing Froude number (*Figure 3*). This was because of smaller water depth at Point C with increasing Froude number which reduced overflow behind the vegetation.

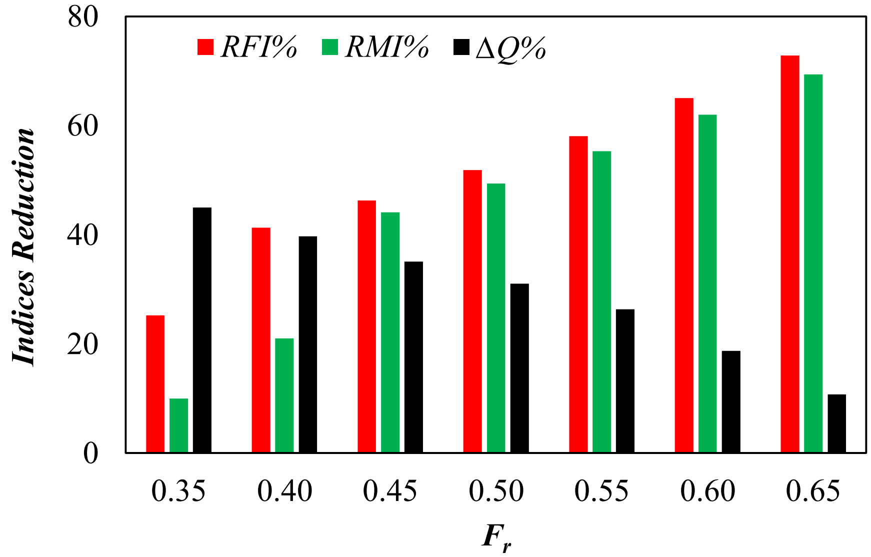

Figure 3. Values of RFI%, RMI%, and ΔQ% for different values of Froude number (F_r)

3.2 ANN-Model Based Result

To predict values of *RFI%, RMI%,* and Δ*Q%*, ANN-model were used to select best fitted model. Each model has two different layer and each layer have different number of neurons. Number of neurons in input layer were kept constant (three) and varied for hidden layer in each model (six and nine neurons). A concept of feed-forward multi-layered Perceptron (*MLP*) was tested for predicting the values of *RFI%, RMI%*, and Δ*Q%*. Various performance indicator such as R^2, *RSME, SSE*, *MAE*, and *NSE* were evaluated. The predicted values of RFI%, RMI% and Δ*Q%* are shown in *Figure 4*. The values of performance indicator such as R^2, *RSME, SSE*, *MAE,* and *NSE* are shown in *Figure 5*. The computed values of R^2, *RSME, SSE*, *MAE*, and *NSE* has also been summarized in Table 2. It was noticed that an ANN-model with nine neuron in a hidden layer was best compared to ANN-model with six neuron in a hidden layer (*Figure 4-5*)(Table-2). In *Figure-5* and Table-2, T and V indicates the training and validation values of the model respectively.

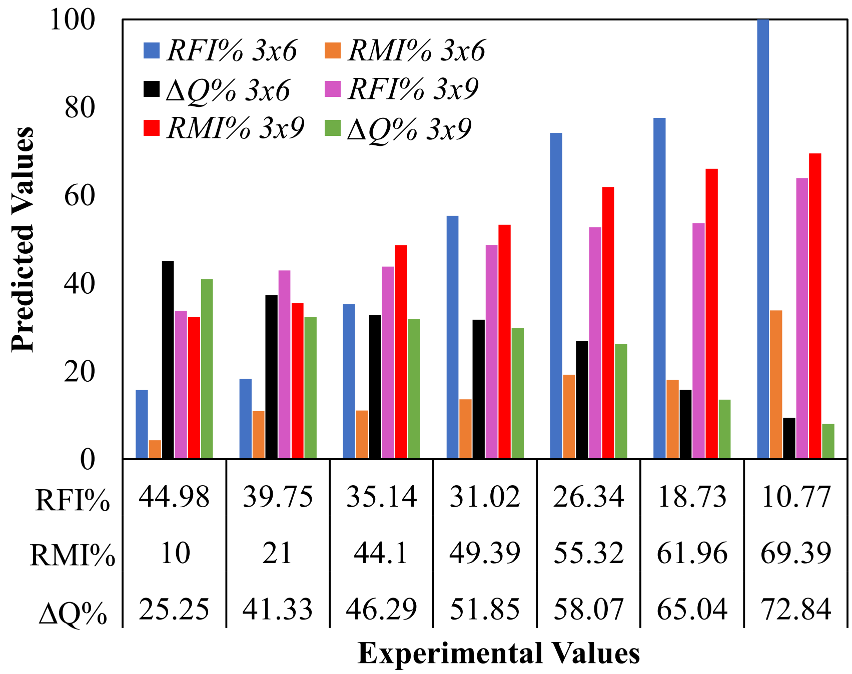

Figure 4. Predicted values of RFI%, RMI%, and ΔQ% by different ANN-model

Table-2 Result of performance indicator by different ANN-model.

	RFI%-ANN-3X6		RFI%-ANN-3X9		RMI%-ANN-3X6		RMI%-ANN-3X9		ΔQ%-ANN-3X6		ΔQ%-ANN-3X9	
	T	V	T	V	T	V	T	V	T	V	T	V
R^2	0.27	0.91	0.91	0.96	0.25	0.4	0.57	0.69	0.78	0.81	0.7	0.89
RMSE	5.25	0.68	2.17	1.59	8.17	2.83	3.57	4.32	3.19	3.39	2.3	3.17
NSE	0.75	0.97	0.72	0.79	0.88	0.61	0.68	0.66	0.88	0.98	1.0	0.92
SSE	11.5	4.42	18.87	7.6	21.7	24.09	51.12	56.18	40.8	34.52	20.3	30.17
MAE	3.49	2.49	1.22	2.55	2.14	4.35	3.16	6.5	5.8	0.3	2.35	3.22

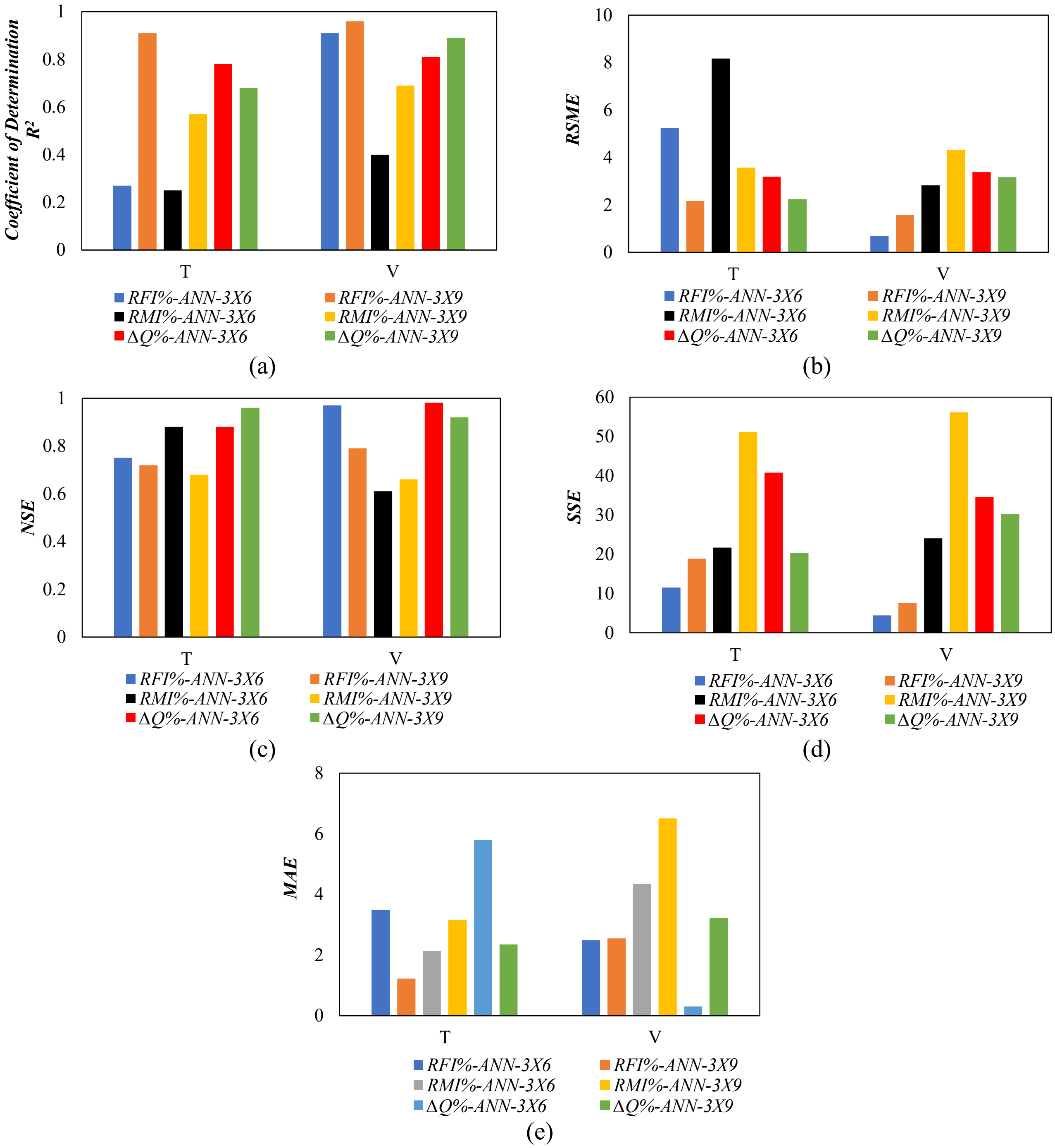

Figure 5. Performance indicator of ANN-model with six and nine neurons in hidden layer

4 CONCLUSIONS

The current research was performed in three different phases to investigate flow parameters such as reduction of fluid force index, moment index, and overflow volume under sub-critical flow conditions. In the first phase of research, experiment was conducted in a laboratory to study these indices at Point G. In the second phase, ANN-based models were tested to evaluate the performance of different model. In last phase some statistical analysis was performed to predict values of indices such as *RFI%, RMI%,* and $\Delta Q\%$ by equation derived. Based on above-mentioned phases following conclusion were conclude from present research.

1. The reduction of fluid force index increased by increasing the Froude number. This was because of increased in water depth at Point C by increasing Froude number. The maximum reduction of fluid force index was noticed to be 73% against the highest value of the Froude number ($Fr = 0.65$).
2. The reduction of moment index increased by increasing the Froude number. This was because of increased in fluid force index at Point C by increasing Froude number. The maximum reduction of moment index was noticed to be 70% against the highest value of the Froude number ($Fr = 0.65$).
3. The reduction of overflow volume decreased by increasing the Froude number. This was because of increased in water depth at Point C by increasing initial water depth. The maximum reduction of overflow volume was noticed to be 45% against the highest value of the Froude number ($Fr = 0.65$).
4. ANN-model with nine different neurons shows best performance with lowered values of R^2 and *NSE* and greater values of *RSE, SSE, MAE* compared to ANN-model with six different neurons.

5 ACKNOWLEDGEMENTS

Author would like to acknowledge Civil Engineering Department of University of Engineering and Technology Taxila for providing laboratory facilities to perform the following research.

REFERENCES

1. van Rooijen A., Lowe R., Ghisalberti M. et al. Predicting current-induced drag in emergent and submerged aquatic vegetation canopies [J]. Frontiers in Marine Science, 2018, 5: 449.
2. Liu C., Nepf H. M. Sediment deposition within and around a finite patch of model vegetation over a range of channel velocity [J]. Water Resources Research, 2016, 52: 600-612.
3. Meng-Yang Liu, Wen-Xin Huai, Zhong-Hua Yang, Yu-Hong Zeng, A genetic programming-based model for drag coefficient of emergent vegetation in open channel flows, Advances in Water Resources, Volume 140, 2020, 103582, ISSN 0309 1708, https://doi.org/10.1016/j.advwatres.2020.103582.

4. Aberle, Jochen; Järvelä, Juha (2013). Flow resistance of emergent rigid and flexible floodplain vegetation. Journal of Hydraulic Research, 51(1), 33–45. https://doi.org/10.1080/00221686.2012.754795.
5. N. Murtaza, G. A. Pasha, and A. Ahmed, "Experimental Investigation of flood energy dissipation for hill torrents management." [Online]. Available: https://www.researchgate.net/publication/373523233.
6. Pasha, G. A., Tanaka, N., Yagisawa, J., & Achmad, F. N. (2017). Tsunami mitigation by combination of coastal vegetation and a backward-facing step. Coastal Engineering Journal, 60(1), 1–22. https://doi.org/10. 1080/21664250.2018.1437014
7. Muhammad Ahmad, Usman Ghani, Naveed Anjum, Ghufran Ahmed Pasha, Muhammad Kaleem Ullah, Afzal Ahmed, Investigating the Flow Hydrodynamics in a Compound Channel with Layered Vegetated Floodplains, 2020, Vol 6, No 5, Civil Engineering Journal, DOI: 10.28991/cej-2020-03091513.
8. Anjum, N., Tanaka, N. Study on the flow structure around discontinued vertically layered vegetation in an open channel. J Hydrodyn 32, 454–467 (2020). https://doi.org/10.1007/s42241-019-0040-2.
9. Y. Peltier, Sébastien Proust, N. Rivière, André Paquier, K. Shiono. Turbulent flows in straight compound open channel with a transverse embankment on the floodplain. Journal of Hydraulic Research, 2013, 51 (4), p. 446 - p. 458. https://doi.org/10.1080/00221686.2013.796499.
10. Sanjou, M, Okamoto, T, Nezu, I. Experimental study on fluid energy reduction through a flood protection forest. J Flood Risk Management. 2018; 11:e12339. https://doi.org/10.1111/jfr3.12339.
11. Valyrakis, M., Liu, D., Turker, U. et al. The role of increasing riverbank vegetation density on flow dynamics across an asymmetrical channel. Environ Fluid Mech 21, 643–666 (2021). https://doi.org/10.1007/s10652-021-09791-9.
12. N. Tanaka, "Effectiveness and Limitation of Coastal Forest in Large Tsunami conditions of Japanese Pine Tree on Coastal Sand Dunes in Tsunami Caused by Greatest East Japan Earthquake," 2012.
13. S. Evangelista, "Experiments and Numerical Simulations of Dike Erosion due to a Wave Impact," Water (Basel), vol. 7, no. 10, pp. 5831–5848, Oct. 2015, doi: 10.3390/w7105831.
14. M. M. Rahman, C. Schaab, and E. Nakaza, "Experimental and Numerical Modeling of Tsunami Mitigation by Canals," J Waterw Port Coast Ocean Eng, vol. 143, no. 1, Jan. 2017, doi: 10.1061/(ASCE)WW.1943-5460.0000355.
15. R. Nateghi, J. D. Bricker, S. D. Guikema, and A. Bessho, "Statistical Analysis of the Effectiveness of Seawalls and Coastal Forests in Mitigating Tsunami Impacts in Iwate and Miyagi Prefectures," PLoS One, vol. 11, no. 8, p. e0158375, Aug. 2016, doi: 10.1371/journal.pone.0158375.
16. G. A. Pasha and N. Tanaka, "Undular hydraulic jump formation and energy loss in a flow through emergent vegetation of varying thickness and density," Ocean Engineering, vol. 141, pp. 308–325, Sep. 2017, doi: 10.1016/j.oceaneng.2017.06.049.
17. W. Kellens, T. Terpstra, and P. De Maeyer, "Perception and Communication of Flood Risks: A Systematic Review of Empirical Research," Risk Analysis, vol. 33, no. 1, pp. 24–49, Jan. 2013, doi: 10.1111/j.1539-6924.2012.01844.x.

18. R. Ali Hasan Muhammad and N. Tanaka, "Energy Reduction of a Tsunami Current through a Hybrid Defense System Comprising a Sea Embankment Followed by a Coastal Forest," Geosciences (Basel), vol. 9, no. 6, p. 247, Jun. 2019, doi: 10.3390/geosciences9060247.
19. K. Pakoksung, A. Suppasri, and F. Imamura, "Systematic Evaluation of Different Infrastructure Systems for Tsunami Defense in Sendai City," Geosciences (Basel), vol. 8, no. 5, p. 173, May 2018, doi: 10.3390/geosciences8050173.
20. Suppasri, N. Shuto, F. Imamura, S. Koshimura, E. Mas, and A. C. Yalciner, "Lessons Learned from the 2011 Great East Japan Tsunami: Performance of Tsunami Countermeasures, Coastal Buildings, and Tsunami Evacuation in Japan," Pure Appl Geophys, vol. 170, no. 6–8, pp. 993–1018, Jun. 2013, doi: 10.1007/s00024-012-0511-7.
21. N. Tanaka, "Vegetation bioshields for tsunami mitigation: review of effectiveness, limitations, construction, and sustainable management," Landscape and Ecological Engineering, vol. 5, no. 1, pp. 71–79, Feb. 2009, doi: 10.1007/s11355-008-0058-z.
22. A. Munir and J. Iqbal, "Flash flood water management practices in Dera Ghazi Khan City (Pakistan): a remote sensing and GIS prospective," Natural Hazards, vol. 81, no. 2, pp. 1303–1321, Mar. 2016, doi: 10.1007/s11069-015-2136-5.
23. A. Munir, S. R. Ahmad, and S. Hafeez, "Integrated Hazard Modeling for Simulating Torrential Stream Response to Flash Flood Events," ISPRS Int J Geoinf, vol. 9, no. 1, p. 1, Dec. 2019, doi: 10.3390/ijgi9010001.
24. P. Peruzzo, F. De Serio, A. Defina, and M. Mossa, "Wave Height Attenuation and Flow Resistance Due to Emergent or Near-Emergent Vegetation," Water (Basel), vol. 10, no. 4, p. 402, Mar. 2018, doi: 10.3390/w10040402.
25. M. Sanjou, T. Okamoto, and I. Nezu, "Experimental study on fluid energy reduction through a flood protection forest," J Flood Risk Manag, vol. 11, no. 4, p. e12339, Dec. 2018, doi: 10.1111/jfr3.12339.
26. N. Anjum, U. Ghani, G. Ahmed Pasha, A. Latif, T. Sultan, and S. Ali, "To Investigate the Flow Structure of Discontinuous Vegetation Patches of Two Vertically Different Layers in an Open Channel," Water (Basel), vol. 10, no. 1, p. 75, Jan. 2018, doi: 10.3390/w10010075.
27. S. Mulahasan and T. Stoesser, "Flow resistance of in-line vegetation in open channel flow," International Journal of River Basin Management, vol. 15, no. 3, pp. 329–334, Jul. 2017, doi: 10.1080/15715124.2017.1307847.
28. M. Ayyoub Tanvir, M. Tahir Siddiqui, A. Hussain Shah, and D. Ghazi Khan-Pakistan, "Growth and Price Trend of Eucalyptus camaldulensis in Central Punjab." [Online]. Available: http://www.ijab.org.
29. G. A. Pasha and N. Tanaka, "Undular hydraulic jump formation and energy loss in a flow through emergent vegetation of varying thickness and density," Ocean Engineering, vol. 141, pp. 308–325, Sep. 2017, doi: 10.1016/j.oceaneng.2017.06.049.
30. A. Ahmed and A. R. Ghumman, "Experimental Investigation of Flood Energy Dissipation by Single and Hybrid Defense System," Water (Basel), vol. 11, no. 10, p. 1971, Sep. 2019, doi: 10.3390/w11101971.

31. S. Lakusic, “Reference water levels for the design of dykes and earthfill dams,” Journal of the Croatian Association of Civil Engineers, vol. 70, no. 3, pp. 225–233, Apr. 2018, doi: 10.14256/JCE.2093.2017.
32. S. A. M. Al-Hashimi, H. M. Madhloom, T. N. Nahi, and N. Al-Ansari, “Channel Slope Effect on Energy Dissipation of Flow over Broad Crested Weirs,” Engineering, vol. 08, no. 12, pp. 837–851, 2016, doi: 10.4236/eng.2016.812076.
33. G. Mahtabi and H. Arvanaghi, “Experimental and numerical analysis of flow over a rectangular full-width sharp-crested weir,” Water Science and Engineering, vol. 11, no. 1, pp. 75–80, Jan. 2018, doi: 10.1016/j.wse.2018.03.004.
34. Ahmed, Afzal, Manousos Valyrakis, Abdul Razzaq Ghumman, Rashid Farooq, Ghufran Ahmed Pasha, Shahmir Janjua, and Ali Raza. 2023. "Experimental and Artificial Neural Network (ANN) Modeling of Instream Vegetation Hydrodynamic Resistance" Hydrology 10, no. 3: 73. https://doi.org/10.3390/hydrology10030073.